A Novel Approach for Characterizing Protein Ligand Complexes: Molecular Basis for Specificity of Small-Molecule Bcl-2 Inhibitors

A Novel Approach for Characterizing Protein Ligand Complexes: Molecular Basis for Specificity of Small-Molecule Bcl-2 Inhibitors

Alexey A. Lugovskoy,[†,‡] Alexei I. Degterev,[§] Amr F. Fahmy,[‡] Pei Zhou,[‡] John D. Gross,[‡] Junying Yuan,[§] and Gerhard Wagner*,[‡,⊥]

Contribution from the Committee on Higher Degrees in Biophysics, Harvard University, Cambridge, Massachusetts 02138, Department of Biochemistry and Molecular Pharmacology, Harvard Medical School, 240 Longwood Avenue, Boston, Massachusetts 02115, and Department of Cell Biology, Harvard Medical School, 240 Longwood Avenue, Boston, Massachusetts 02115

Abstract: The increasing diversity of small molecule libraries has been an important source for the development of new drugs and, more recently, for unraveling the mechanisms of cellular events—a process termed chemical genetics.[1] Unfortunately, the majority of currently available compounds are mechanism-based enzyme inhibitors, whereas most of cellular activity regulation proceeds on the level of protein–protein interactions. Hence, the development of small molecule inhibitors of protein–protein interactions is important. When screening compound libraries, low-micromolar inhibitors of protein interactions can be routinely found. The enhancement of affinities and rationalization of the binding mechanism require structural information about the protein–ligand complexes. Crystallization of low-affinity complexes is difficult, and their NMR analysis suffers from exchange broadening, which limits the number of obtainable intermolecular constraints. Here we present a novel method of ligand validation and optimization, which is based on the combination of structural and computational approaches. We successfully used this method to analyze the basis for structure–activity relationships of previously selected [2] small molecule inhibitors of the antiapoptotic protein Bcl-xL and identified new members of this inhibitor family.

Introduction

Apoptosis is a process of tightly regulated energy-dependent cellular suicide, and it plays a critical part in the homeostasis of multicellular organisms.[3,4] Inhibition of apoptosis has been shown to contribute to the processes of tumorogenesis and development of chemoresistance.[3–10] In recent years molecular mechanisms of apoptosis have been investigated, and the members of the Bcl-2 family have emerged as key regulators of apoptotic pathways. The levels of the antiapoptotic Bcl-2 family proteins are often elevated in a variety of tumors, which plays a major role in chemoresistance and contributes to poor cancer prognosis.[3,6,9] On the other hand, proapoptotic family members, such as Bax,[11,12] Noxa,[13] and PUMA, [14] are tran-

scriptionally activated by the tumor suppressor p53. Furthermore, recent genetic studies have demonstrated that inactivation of Bax may directly lead to tumorogenesis.[11,15]

Homo- and heterodimerization of Bcl-2 family members through their BH3 domains is the key mechanism regulating the function of these proteins.[16–21] Synthetic BH3 domain-containing peptide induces apoptosis in oocyte lysates, cultured cells, and in vivo xenografts of human leukemia HL-60 cells.[18,22,23] Recently Degterev et al.[2] have selected a series of

† Committee on Higher Degrees in Biophysics.
‡ Department of Biochemistry and Molecular Pharmacology.
§ Department of Cell Biology.
⊥ Phone: (617) 432–3213. Fax: (617) 432–4383. E-mail: gerhard_wagner@hms.harvard.edu.

(1) Stockwell, B. R. *Trends Biotechnol.* **2000**, *18*, 449–55.
(2) Degterev, A.; Lugovskoy, A.; Cardone, M.; Mulley, B.; Wagner, G.; Mitchison, T.; Yuan, J. *Nat. Cell Biol.* **2001**, *3*, 173–182.
(3) Rudin, C. M.; Thompson, C. B. *Annu. Rev. Med.* **1997**, *48*, 267–81.
(4) Thompson, C. B. *Science* **1995**, *267*, 1456–62.
(5) Chresta, C. M.; Hickman, J. A. *Urol. Res.* **1999**, *27*, 1–2.
(6) Decaudin, D.; Marzo, I. I.; Brenner, C.; Kroemer, G. *Int. J. Oncol.* **1998**, *12*, 141–52.
(7) Hager, J. H.; Hanahan, D. *Ann. N.Y. Acad. Sci.* **1999**, *887*, 150–63.
(8) Reed, J. C. *Toxicol. Lett.* **1995**, *82–83*, 155–8.
(9) Reed, J. C. *Hematol. Oncol. Clin. N. Am.* **1995**, *9*, 451–73.
(10) Wyllie, A. H.; Bellamy, C. O.; Bubb, V. J.; Clarke, A. R.; Corbet, S.; Curtis, L.; Harrison, D. J.; Hooper, M. L.; Toft, N.; Webb, S.; Bird, C. C. *Br. J. Cancer* **1999**, *80 Suppl 1*, 34–7.
(11) McCurrach, M. E.; Connor, T. M.; Knudson, C. M.; Korsmeyer, S. J.; Lowe, S. W. *Proc. Natl. Acad. Sci. U.S.A.* **1997**, *94*, 2345–9.
(12) Matsuyama, S.; Schendel, S. L.; Xie, Z.; Reed, J. C. *J. Biol. Chem.* **1998**, *273*, 30995-1001.
(13) Oda, E.; Ohki, R.; Murasawa, H.; Nemoto, J.; Shibue, T.; Yamashita, T.; Tokino, T.; Taniguchi, T.; Tanaka, N. *Science* **2000**, *288*, 1053–8.
(14) Nakano, K. a. V., K. H. *Mol. Cell* **2001**, *7*, 683–694.
(15) Zhang, L.; Yu, J.; Park, B. H.; Kinzler, K. W.; Vogelstein, B. *Science* **2000**, *290*, 989–92.
(16) Simonen, M.; Keller, H.; Heim, J. *Eur. J. Biochem.* **1997**, *249*, 85–91.
(17) Zha, J.; Harada, H.; Osipov, K.; Jockel, J.; Waksman, G.; Korsmeyer, S. J. *J. Biol. Chem.* **1997**, *272*, 24101–4.
(18) Holinger, E. P.; Chittenden, T.; Lutz, R. J. *J. Biol. Chem.* **1999**, *274*, 13298–304.
(19) Minn, A. J.; Kettlun, C. S.; Liang, H.; Kelekar, A.; Vander Heiden, M. G.; Chang, B. S.; Fesik, S. W.; Fill, M.; Thompson, C. B. *Embo J.* **1999**, *18*, 632–43.
(20) Wang, K.; Gross, A.; Waksman, G.; Korsmeyer, S. J. *Mol. Cell. Biol.* **1998**, *18*, 6083–9.
(21) Gross, A.; Jockel, J.; Wei, M. C.; Korsmeyer, S. J. *Embo J.* **1998**, *17*, 3878–85.
(22) Cosulich, S. C.; Worrall, V.; Hedge, P. J.; Green, S.; Clarke, P. R. *Curr. Biol.* **1997**, *7*, 913–20.
(23) Wang, J. L.; Zhang, Z. J.; Choksi, S.; Shan, S.; Lu, Z.; Croce, C. M.; Alnemri, E. S.; Korngold, R.; Huang, Z. *Cancer Res.* **2000**, *60*, 1498–502.
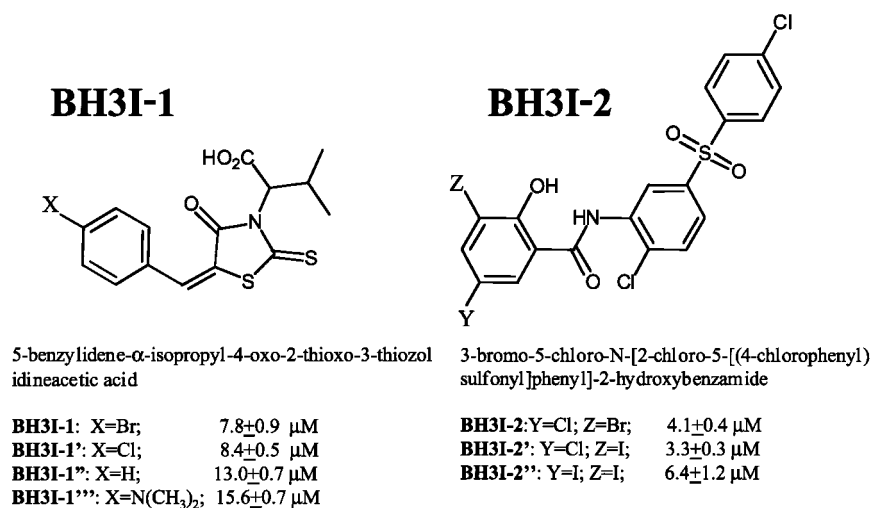
Figure 1. Structures and affinities toward Bcl-xL of the two classes of BH3Is previously described.[2]

small molecule inhibitors (termed BH3Is) which specifically antagonize the BH3 domain-mediated interaction between anti- and proapoptotic members of the Bcl-2 family. BH3Is induce apoptosis in a broad range of cells, in a manner which depends on their ability to disrupt the BH3 domain mediated protein−protein interactions. By using NMR titrations, we examined the BH3I/Bcl-xL complex and demonstrated that BH3Is bind to the same hydrophobic groove as the Bak BH3 peptide, hence, acting as small molecule mimetics of the proapoptotic BH3 domain.

Characterization of the molecular geometry of protein−compound complexes is central to our understanding of structure−activity relationships and subsequent chemical optimization.[24] Ideally, this is achieved with experimental methods, such as crystallography or NMR.[25] However, crystallization of low-affinity complexes is difficult, and NMR analysis of such complexes suffers from exchange broadening, limiting the number of intermolecular constraints obtainable. Moreover, current developments in the field of combinatorial chemistry and chemical genetics require methods capable of analyzing multiple interactions in a high-throughput format. Computational techniques that use the structure of the free protein and the topology of the compound present a tempting tool to facilitate such efforts. Additionally, virtual screening approaches that can be used to guide chemical modifications would be extremely useful. However, the computed hypothetical complex structures require experimental verification, ideally with less effort than that of full experimental structure analysis. Therefore, use of validated computational approaches can result in a rapid assessment of the bound state and optimization of the ligand.[26]

The majority of the molecular modeling approaches[27−31] utilize stochastic search procedures, such as Monte Carlo or simulated annealing. Since these methods do not enumerate all of the relative configurations of the molecules, they may fail to yield the most favorable orientation. Therefore, an exhaustive search of the conformational space at high resolution would be preferable. Unfortunately, due to the fact that interaction interfaces on proteins are relatively large, exhaustive searches are usually computationally costly. Thus, there is a great need for new creative computational approaches to address this problem. Furthermore, ways to limit the search space with experimental data would be desirable.

In this paper we present a novel method for ligand validation and optimization based on a combination of structural and computational approaches. We use NMR chemical shift perturbation as an efficient tool for rapid mapping of interaction interfaces[32,33] and direct NMR-derived constraints to restrict the conformational space for molecular modeling routines. As a molecular modeling module, we utilized the novel program TreeDock,[34] which is optimized to allow high-resolution exhaustive enumeration of all relative orientations between complex components. It uses the Lennard-Jones potential as the scoring function to obtain the protein−compound complexes based primarily on shape complementarity. The models of complexes were validated through an independent set of NMR restraints.

We employed this method to analyze structure−activity relationships in the BH3Is/Bcl-xL complexes. We found that the free energies of the complexes calculated using the TreeDock routine correlated well with in vitro Bcl-xL binding affinities of the compounds. To validate our method further, we experimentally tested the affinities of two close homologues of the original compounds, which scored low in our algorithm, and found that they did not bind to Bcl-xL. Finally, we performed a virtual screening of BH3Is homologues in the Chemnavigator (www.chemnavigator.com) and Chembridge (www.hit2lead.com) compound libraries and identified an additional compound-inhibitor of the Bcl-xL/BH3 interaction.

Results and Discussion

BH3Is Bind to and Stabilize an "Open-Cleft" Conformation of Bcl-xL. To understand the structural determinants of

(24) Tollenaere, J. P. *Pharm. World Sci.* **1996**, *18*, 56−62.
(25) Zheng, T. S. *Nat. Cell. Biol.* **2001**, *3*, E43−6.
(26) Blundell, T. L. *Nature* **1996**, *384*, 23−6.
(27) Verlinde, C. L.; Hol, W. G. *Structure* **1994**, *2*, 577−87.
(28) Strynadka, N. C.; Eisenstein, M.; Katchalski-Katzir, E.; Shoichet, B. K.; Kuntz, I. D.; Abagyan, R.; Totrov, M.; Janin, J.; Cherfils, J.; Zimmerman, F.; Olson, A.; Duncan, B.; Rao, M.; Jackson, R.; Sternberg, M.; James, M. N. *Nat. Struct. Biol.* **1996**, *3*, 233−9.
(29) Sternberg, M. J.; Gabb, H. A.; Jackson, R. M. *Curr. Opin. Struct. Biol.* **1998**, *8*, 250−6.
(30) Sternberg, M. J.; Aloy, P.; Gabb, H. A.; Jackson, R. M.; Moont, G.; Querol, E.; Aviles, F. X. *Ismb* **1998**, *6*, 183−92.
(31) Zeng, J. *Comb. Chem. High Throughput Screen.* **2000**, *3*, 355−62.

(32) Markus, M. A.; Nakayama, T.; Matsudaira, P.; Wagner, G. *Protein Sci.* **1994**, *3*, 70−81.
(33) Shuker, S. B.; Hajduk, P. J.; Meadows, R. P.; Fesik, S. W. *Science* **1996**, *274*, 1531−4.
(34) Fahmy, A.; Wagner, G. *J. Am. Chem. Soc.* **2002**, *124*, 1241−1250.
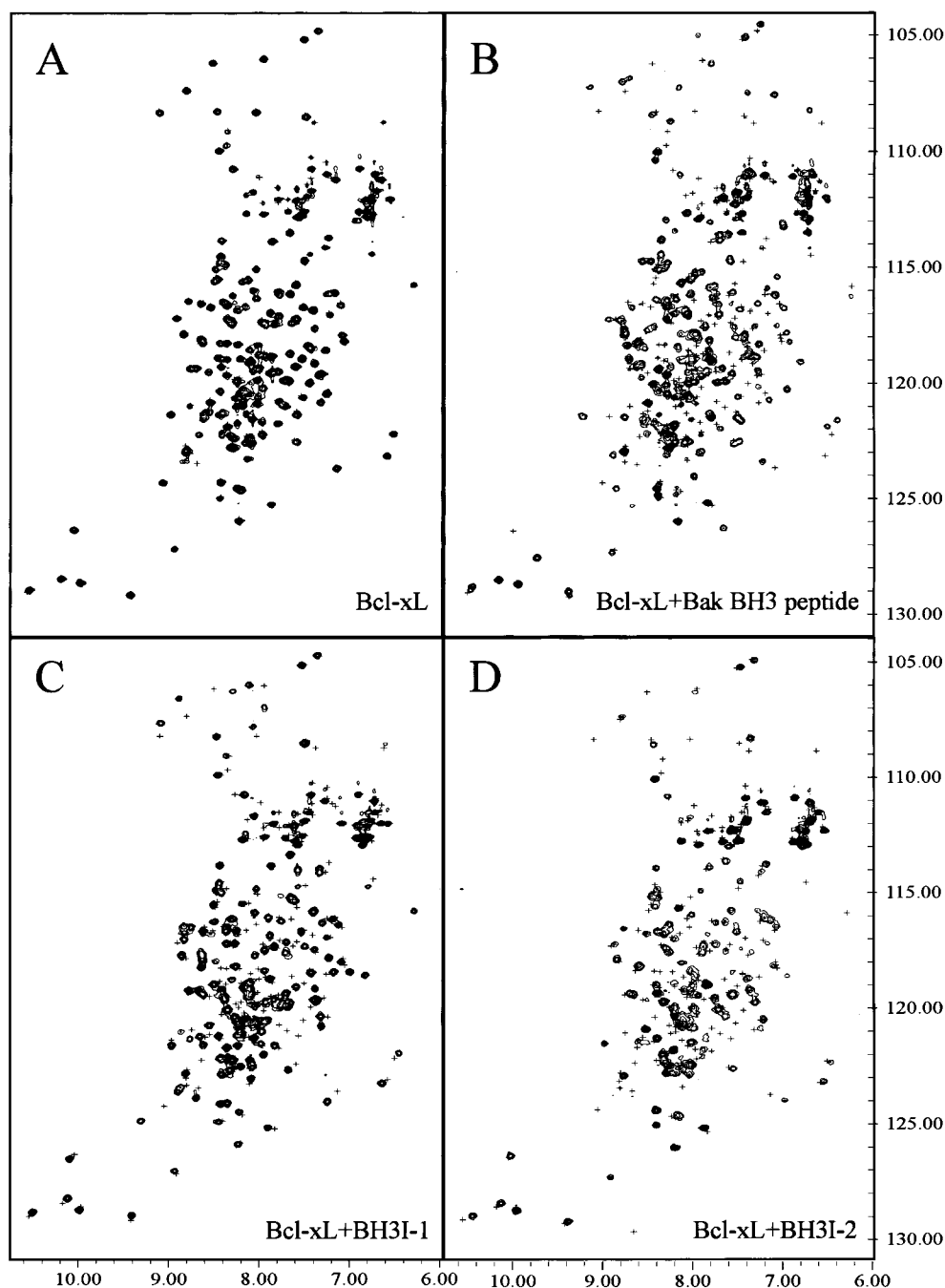
Figure 2. NMR titration experiments. (A) $^1H-^{15}N$ HSQC spectra of free Bcl-xL. (B) $^1H-^{15}N$ HSQC spectra of Bcl-xL with 2-fold excess of Bak BH3 peptide. (C) $^1H-^{15}N$ HSQC spectra of Bcl-xL with 2-fold excess of BH3I-1. (D) $^1H-^{15}N$ HSQC spectra of Bcl-xL with 2-fold excess of BH3I-2. The cross-peak positions in free Bcl-xL are indicated with "+" marks.

action among the previously identified BH3Is (Figure 1) we decided to characterize the interface between individual compounds and Bcl-xL. For this purpose we employed NMR spectroscopy titration techniques, which are capable of detecting interactions with affinities up to 10 mM.[32] Analyses of changes in 2D $^{15}N/^1H$ heteronuclear single quantum correlation spectra (HSQC)[35] of ^{15}N-labeled Bcl-xL upon addition of the inhibitors revealed that all seven BH3Is induced significant changes in the Bcl-xL structure. These perturbations were similar to that induced by Bak BH3 peptide (Figure 2 and data not shown), which is known to facilitate the formation of the hydrophobic

groove between BH1, BH3, and BH2 domains of the protein.[36] Therefore, a similar grove is formed upon additions of BH3Is.[2] Since approximately a third of the protein amide proton resonances changed upon addition of the molecules, we reasoned that it would be beneficial to separate changes in chemical environment due to the conformational switch from those due to direct interactions with the compounds. We decided to take advantage of the fact that BH3Is fall into two distinct structural classes (Figure 1) with members within each class differing in a single substituent and compared changes in spectra induced

(35) Bodenhausen, G.; Ruben, D. J. *Chem. Phys. Lett.* **1980**, *69*, 185−189.

(36) Sattler, M.; Liang, H.; Nettesheim, D.; Meadows, R. P.; Harlan, J. E.; Eberstadt, M.; Yoon, H. S.; Shuker, S. B.; Chang, B. S.; Minn, A. J.; Thompson, C. B.; Fesik, S. W. *Science* **1997**, *275*, 983−6.
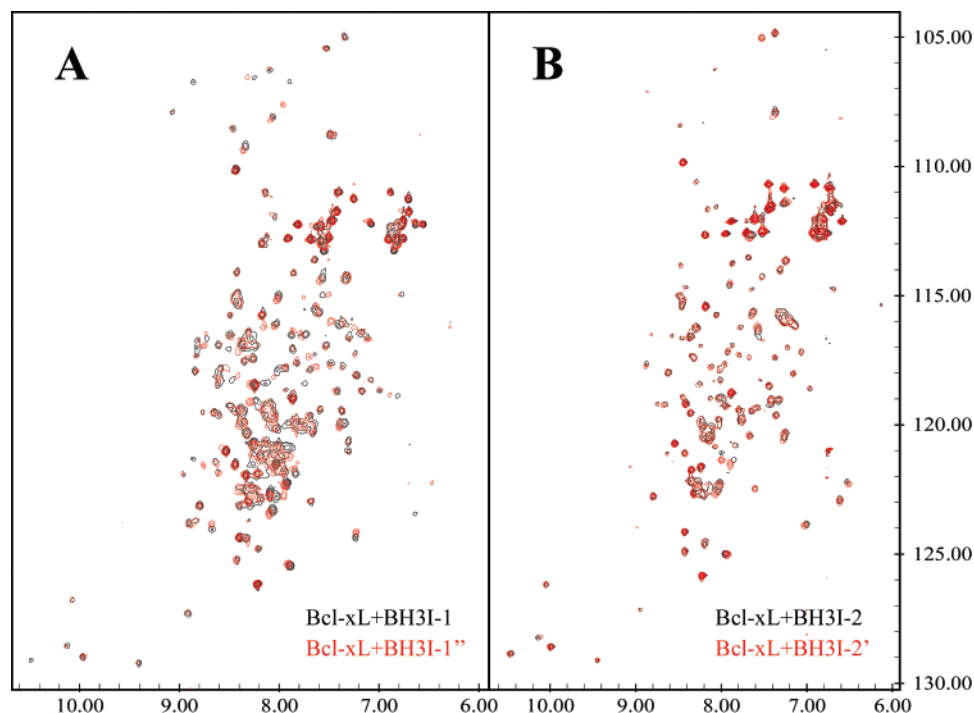
Figure 3. Differential titration experiments. (A) An overlay of $^1H-^{15}N$ HSQC spectra of Bcl-xL with 2-fold excess of BH3I-1 (black) and $^1H-^{15}N$ HSQC spectra of Bcl-xL with 2-fold excess of BH3I-1″ (red). (B) An overlay of $^1H-^{15}N$ HSQC spectra of Bcl-xL with 2-fold excess of BH3I-2 (black) and $^1H-^{15}N$ HSQC spectra of Bcl-xL with 2-fold excess of BH3I-2′ (red).

by various compounds in each of the classes. Since compounds that differ by a single substitution have similar biological activity[2] and bind the same conformational state of Bcl-xL, the only resonances affected differently between the spectra should be in the immediate vicinity of the compound. Indeed, such differential mappings resulted in identification of 8 residues (N100, G102, I104, A106, F110, G111, G112, and R55) between BH3I-1 and BH3I-1″ and 4 residues (F110, A164, A165, R168) between BH3I-2 and BH3I-2′ (Figure 3) as located next to the altered substituents. To obtain a separate set of constraints, we searched for NOE contacts between BH3I-1 and Bcl-xL in a ^{14}N-filtered ^{15}N-edited NOESY−HSQC spectrum. According to this experiment, the benzene ring of the BH3I-1 class lies in the immediate vicinity of amide protons of Y65 and F107. Interestingly, the majority of these hydrophobic residues are buried in the structure of free Bcl-xL,[37] but become accessible to the ligand in the structure of Bcl-xL/Bak BH3 complex.[36] This change in residue accessibility is a direct consequence of the cleft opening conformational change observed upon binding of the BH3 peptide (Figure 4). Therefore, we concluded that BH3Is bind to and stabilize an "open cleft" conformation of Bcl-xL, similar to the Bak BH3 peptide.

Molecular Modeling of BH3Is/Bcl-xL Complexes Reveals the Basis for Structure−Activity Relationship in the Compound Series. Next, we decided to generate molecular models of Bcl-xL/BH3Is complexes based on the structure of Bcl-xL/Bak BH3 peptide complex[36] and obtained interface mapping data. For this purpose we utilized a novel molecular modeling routine TreeDock,[34] which samples exhaustively all of the available conformational space with high (no atom moves more than 1 Å in one step) resolution using the Lennard-Jones

potential as the only scoring function. The fact that BH3Is bind to and stabilize the "open cleft" conformation of Bcl-xL, which has been already structurally characterized,[36] allowed us to keep the protein molecule rigid. We assumed that "open-cleft" conformation of the Bcl-xL/Bak complex represents the protein state of interest. The flexibility of a compound was explored by virtue of docking multiple compound conformers (2−4 per rotatable bond). In cases when structural data on the ligand-binding state of the protein is unavailable, it is advisable to use multiple protein states different by rotamers of few side chains located on the characterized epitope (which is usually small for protein/small molecule interaction). Here we used the following procedure:

In the first step, we choose all solvent-accessible atoms within a 6 Å distance from differentially affected (see Figure 4) amide protons on Bcl-xL as anchor points. This step is required to restrict the spatially accessible space, enabling the use of a systematic search routine. Next, each anchor point was brought into contact with an atom on the compound as a docking point, and the compound was rotated systematically in 3D excluding the areas of van der Waals clashes, with energy being computed for each nonclashing configuration. This procedure was repeated until all possible pairs of anchor points and docking points were explored.

In the second step of the algorithm we clustered the models compliant with interface mapping data, which required all the differentially affected amide protons of Bcl-xL to lie in the vicinity of the compound. Eventually, we took the lowest energy structure out of the cluster that satisfied the criteria. Once identified, the docking point was kept the same for all compounds in the series. The complexes of BH3I-1 and BH3I-2 with Bcl-xL modeled using this approach are presented in Figure 5.

(37) Muchmore, S. W.; Sattler, M.; Liang, H.; Meadows, R. P.; Harlan, J. E.; Yoon, H. S.; Nettesheim, D.; Chang, B. S.; Thompson, C. B.; Wong, S. L.; Ng, S. L.; Fesik, S. W. *Nature* **1996**, *381*, 335−41.
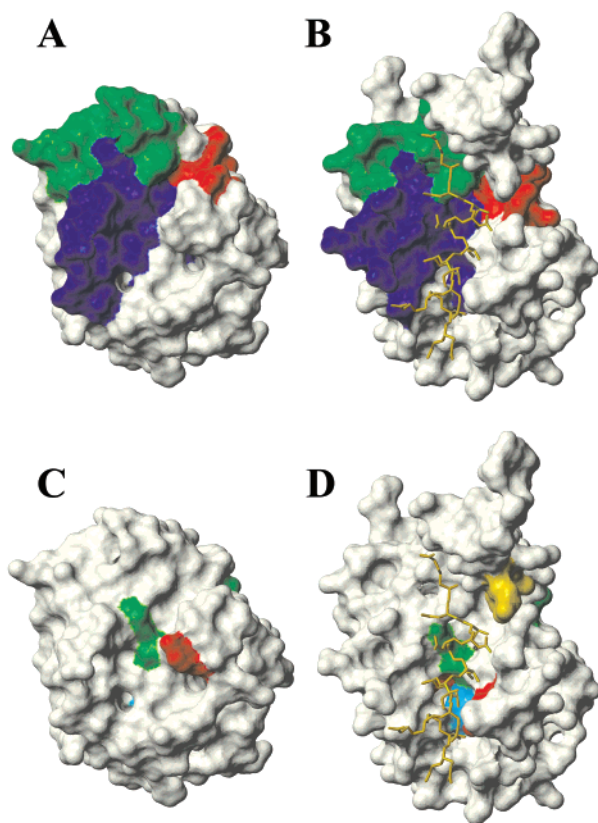
Figure 4. BH3Is/Bcl-xL interaction interface. (A) Structure of free Bcl-xL.[37] Location of the hydrophobic cleft is shown: BH1, dark blue; BH2, green; BH3, red. (B) Structure of Bcl-xL in complex with the Bak BH3 peptide.[36] Location of BH1, BH2, and BH3 domains is shown: BH1, dark blue; BH2, green; BH3, red. (C, D) Differential mapping of BH3I-1 and BH3I-2 analogues binding. Residues differentially affected by the binding of BH3I-1 and BH3I-1″ chemicals are shown in green. Y65 and F107 forming a direct contact with BH3I-1 are shown in red. Residues differentially affected by the binding of BH3I-2 and BH3I-2′ chemicals are shown in gold. F110, which is differentially affected by either BH3I-1 and BH3I-1″, or BH3I-2 and BH3I-2′ is shown in cyan. Residues, such as F107 (red), F110 (cyan), A164, A165, R168 (gold), etc., are buried in the structure of free Bcl-xL (C) and are exposed in the structure of the Bcl-xL complex with the Bak BH3 peptide (D).
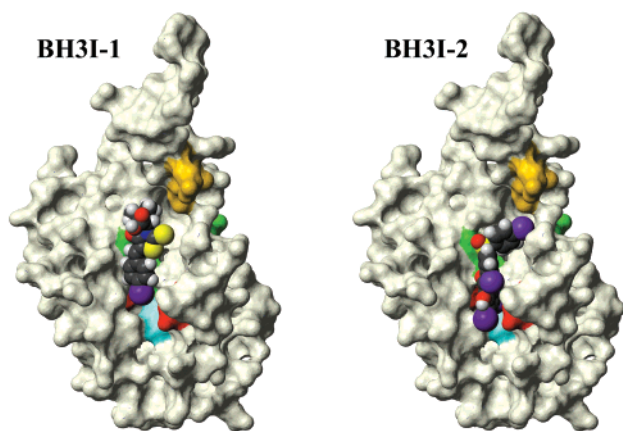

Figure 5. Structural models of BH3I-1/Bcl-xL (on the left) and BH3I-2/Bcl-xL (on the right) complexes.

Using the obtained models we were able to examine the structure−activity relationship for the compounds. In our previous study we found the order of the in vitro affinities and in vivo activities to be BH3I-2′ > BH3I-2 > BH3I-2″ > BH3I-1
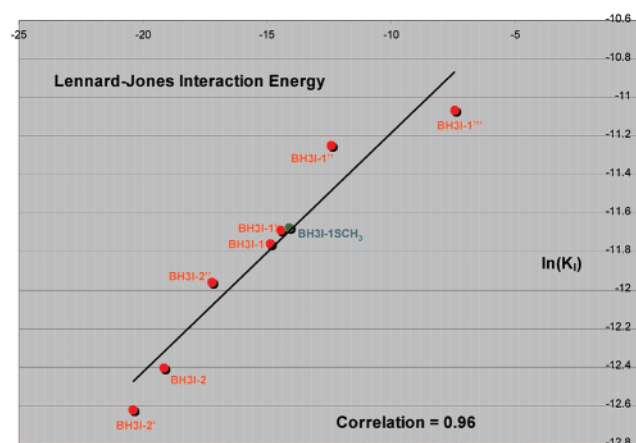
Figure 6. A correlation plot between computed interaction energies in BH3Is/Bcl-xL complexes and their affinities toward Bcl-xL. Data points for BH3Is are shown in red, except for BH3I-1-SCH₃, which is shown in green. Only compounds that bind to Bcl-xL are shown.
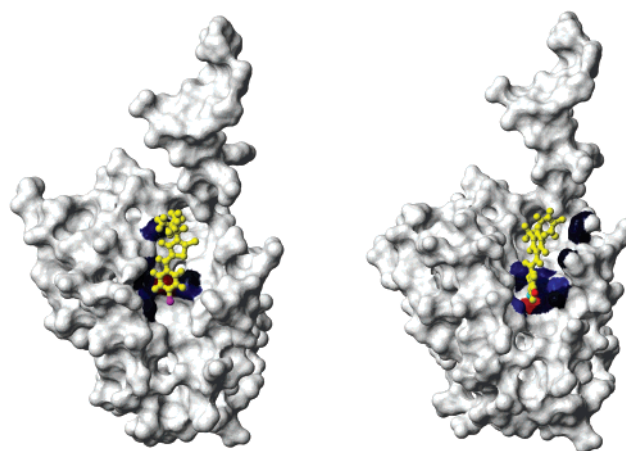

Figure 7. The map of BH3Is binding moieties on the surface of Bcl-xL. The mutual orientation of molecules is the same as in Figure 5. The backbones of the compounds are shown in yellow. Bromine of BH3I-1 (on the left) is colored in magenta. Essential chlorine of BH3I-2 (on the right) is colored in cyan. Bromine of BH3I-2 (on the right) is colored in red. Protein is colored according to normalized contribution of its atoms to BH3Is binding, with white (RGB palette 0 0 0) meaning no interaction, and blue (RGB palette 0 0 1) designating maximal interaction. Anchor points on the protein are shown in red.

> BH3-I-1′ > BH3I-1″ > BH3I-1‴.[2] The compounds scored in exactly the same order in our algorithm, and calculated energies correlated well with the in vitro affinities (Figure 6). Inhibitors of the BH3I-1 class interact mostly with Phe61, Leu94, Gly102, Ala106, Tyr 159, and the aliphatic part of Arg 103 side chain. The bromine group of BH3I-1 (Figure 7 on the left in magenta) interacts with the $C\epsilon_1$ and $H\epsilon_1$ of Phe 61 and $C\gamma_1$, $C\delta_1$, and $C\delta_2$ of Leu94. When bromine is substituted by chlorine (BH3I-1′) or hydrogen (BH3I-1″), these interactions are progressively weakened, resulting in a decrease in the affinity. On the other hand, introduction of a dimethylamine moiety (BH3I-1‴) causes steric clashes between this group and methyl groups ($C\delta_1$ and $C\delta_2$) of Leu94, as well as the ring ($C\delta_1$) of Tyr65, making this compound a poor binder.

Inhibitors of the BH3I-2 class target a longer stretch of the groove centered at residues Phe61, Arg64, Tyr65, Phe69, Leu72, Val90, Ala106, and Phe110. The bromine substituent of BH3I-2 (Figure 7 on the right in red) interacts with the side chain of

Tyr 65, and substitution of this group by iodine (BH3I-2′) strengthens this contact and introduces a new one between iodine and $C\gamma_1$ of Val90. Another important moiety, chlorine in position 5 (Figure 7 on the right in cyan), interacts with the side chain of Phe110, $C\gamma_1$ of Val90, $C\delta_2$ of Leu72, $C\beta$ and carbonyl of Ala106, and $C\epsilon_1$ and $H\epsilon_1$ of Phe 61. The substitution of this chlorine by iodine (BH3I-2″) results in clashes with side chains of Phe110 and Phe61 and, hence, decreases the affinity of the compound.

Since we were able to generate models of BH3Is/Bcl-xL complexes, which provide a structure—activity relationship consistent with experimentally determined compound affinities, we concluded that the described approach yielded valid representations of these complexes. This conclusion is further strengthened by the close proximity of $H\epsilon$ protons on the benzene ring of the BH3I-1 and HN groups of Phe107 and Phe65 in our model, which is compliant with the experimentally observed intermolecular NOEs, which were not used to restrain the modeling procedure.

Rapid Computational Screening of Compound Libraries. The close correlation between in vitro affinities of BH3Is and the computed interaction energy allowed us to set up a virtual screening of available online compound libraries. Indeed, we can utilize the linearity of the correlation plot (Figure 6) to extend our structure—activity relationship analyses to other classes of BH3Is in a high-throughput fashion. Therefore, we selected a total of 93 compounds based on their similarity to BH3Is (more than 80%) and solubility (log P less than 6.0) from Chembridge (www.hit2lead.com) and Chemnavigator (www.chemnavigator.com) libraries. To incorporate ligand flexibility, we varied nonfixed dihedral angles in the compounds and superimposed their backbones with the ones of the structurally closest BH3Is. Finally, we used the TreeDock module to calculate the interaction energy of these compounds with Bcl-xL keeping the same anchoring—docking atom pair as was used in the modeling of the structurally closest BH3I compound.

From this screen, we selected a novel analogue of BH3I-1, which we termed BH3I-1SCH₃ (Figure 8A). Even though it features substitutions in both aliphatic and benzene parts of the compound, it is predicted to have similar affinity to BH3I-1 due to self-compensatory effects of both substitutions. We tested the in vitro binding affinity of this compound to Bcl-xL by a fluorescence polarization assay[2] and an NMR titration experiment. The results indicated that the compound binds Bcl-xL with affinity comparable to that of BH3I-1. Furthermore, its in vitro binding affinity correlated well with calculated Lennard-Jones interaction energy (Figure 6). On the structural level, BH3I-1SCH₃ loses a part of favorable contacts with side chains of Phe61 and Leu94 but gains interactions with Ala164 and Ser167 due to long extension with a methionine-type side chain. Interestingly, Ala164 was affected in differential titration experiments for the BH3I-2, suggesting that BH3I-1SCH₃ provides a possible link between two classes of BH3Is and is of interest for further BH3Is optimization.

To further confirm the ability of our method to select for Bcl-xL binding compounds, we tested the affinities of two close structural homologues of the BH3Is (one for each classs), which scored low in our algorithm during virtual screening (Figure 8B). We tested their in vitro affinity toward Bcl-xL experimen-
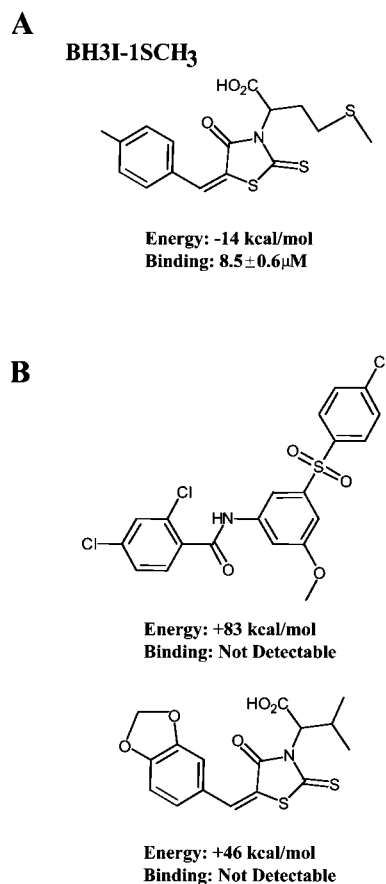
A

BH3I-1SCH₃

Energy: -14 kcal/mol
Binding: 8.5±0.6μM

B

Energy: +83 kcal/mol
Binding: Not Detectable

Energy: +46 kcal/mol
Binding: Not Detectable

Figure 8. The results of virtual screening of small molecule libraries. (A) Structure, interaction energy, and affinity toward Bcl-xL of BH3I-1SCH₃. (B) Structure, interaction energy, and lack of affinity toward Bcl-xL in predicted BH3Is analogues.

tally by the fluorescence polarization assays and NMR titrations and verified that they did not bind to Bcl-xL (data not shown). These experiments altogether demonstrate that our algorithm can be successfully used to computationally screen small-molecule libraries and reliably score the analogues of the compounds of interest.

Conclusions

In this study we have developed a novel approach to ligand validation and optimization, which consists of structural interface mapping combined with an exhaustive computational interaction analysis technique. We successfully utilized this method to reveal the specificity determinants for structure—activity relationships of small-molecule inhibitors of antiapoptotic Bcl-2 proteins. Additionally, we performed a virtual screen of two small compound libraries and identified a new small molecule inhibitor of Bcl-xL. With the number of available macromolecular structures[26] and small-molecule diversity[1] growing rapidly, there is a great need for reliable computational ways to analyze protein—compound interactions. We believe that our approach can be successfully used for analysis of structure—activity relationships in protein—ligand complexes.

Experimental Section

Plasmid Construction. Bcl-xL-His₆ bacterial expression vector was generated as previously described.[36]

NMR Spectroscopy. Sequential assignments were achieved as previously described.[38] ¹H—¹⁵N HSQC spectra were recorded by adding

different amounts of BH3Is and Bak BH3 peptide into 300 μM ^{15}N-labeled Bcl-xL/His. The determination of the BH3Is affinities toward Bcl-xL was performed as previously described.[39] NOE transfers between BH3I-1 and Bcl-xL were observed in the ^{14}N-filtered ^{15}N-edited NOESY−HSQC recorded on 100% deuterated Bcl-xL in H$_2$O according to ref 40 with the exception that the ^{1}H evolution period was replaced with a semiconstant time[41] element and the phase of the second proton 90° pulse is adjusted to select protons that are not coupled to ^{15}N.

Fluorescence Polarization Assay. The Bak BH3 peptide (Research Genetics) was labeled using NHS-Oregon Green (Molecular Probes) and purified by HPLC. Fluorescence polarization assays containing labeled BH3 peptide and Bcl-xL-His$_6$ fusion protein, which was previously utilized to characterize BH3/Bcl-xL binding,[36] were performed as previously described [2]. K_D and K_I determinations were performed as previously described.[42]

Calculations of Protein−Compound Interactions. TreeDock module was implemented as a C-program on a single SGI R10K workstation. The input to TreeDock consists of two PDB-files, one for each molecule. Following the coordinates of each atom in a PDB file, its solvent accessible surface is stored. The output of TreeDock is stored in two files: one contains the coordinates of the complex and another (optional) records Lennard-Jones energy contribution of all chemical moieties. Parameters for the Lennard-Jones potential were obtained from the X-PLOR program[43,44] The TreeDock module is described in the accompanying paper.[34] TreeDock module was able to reconstruct the taken apart Bcl-xL/BH3 complex with a high (less than 1 Å RMSD) precision.

(38) Lugovskoy, A. A.; Zhou, P.; Chou, J. J.; McCarty, J. S.; Li, P.; Wagner, G. *Cell* **1999**, *99*, 747−55.
(39) Johnson, P. E.; Tomme, P.; Joshi, M. D.; McIntosh, L. P. *Biochemistry* **1996**, *35*, 13895−906.
(40) Talluri, S.; Wagner, G. *J. Magn. Reson. B* **1996**, *112*, 200−5.
(41) Grzesiek, S.; Bax, A. *J. Biomol. NMR* **1993**, *3*, 185−204.
(42) Dandliker, W. B.; Hsu, M. L.; Levin, J.; Rao, B. R. *Methods Enzymol.* **1981**, *74*, 3−28.
(43) Brunger, A. T.; Adams, P. D.; Clore, G. M.; DeLano, W. L.; Gros, P.; Grosse-Kunstleve, R. W.; Jiang, J. S.; Kuszewski, J.; Nilges, M.; Pannu, N. S.; Read, R. J.; Rice, L. M.; Simonson, T.; Warren, G. L. *Acta Crystallogr., Sect. D: Biol. Crystallogr.* **1998**, *54*, 905−21.
(44) Engh, R. A.; Huber, R. *Acta Crystallogr.* **1991**, *A47*, 392−400.